OXFORD

Human Molecular Genetics, 2018, Vol. 27, No. 8 1332–1342

doi: 10.1093/hmg/ddy042
Advance Access Publication Date: 1 February 2018
Original Article

ORIGINAL ARTICLE

Hippocampal mutant APP and amyloid beta-induced cognitive decline, dendritic spine loss, defective autophagy, mitophagy and mitochondrial abnormalities in a mouse model of Alzheimer's disease

Maria Manczak[1,5], Ramesh Kandimalla[1,4], Xiangling Yin[1] and P. Hemachandra Reddy[1,2,3,4,5,6,7,*]

[1]Garrison Institute on Aging, Texas Tech University Health Sciences Center, 3601 4th Street, MS 9424, Lubbock, TX 79430, USA, [2]Garrison Institute on Aging, South West Campus, Texas Tech University Health Sciences Center, 6630 S. Quaker Suite E, MS 7495, Lubbock, TX 79413, USA, [3]Cell Biology and Biochemistry Department, [4]Pharmacology and Neuroscience Department, [5]Neurology Department, [6]Speech, Language and Hearing Sciences Department, Texas Tech University Health Sciences Center, 3601 4th Street, MS 9424, Lubbock, TX 79430, USA and [7]Department of Public Health, Graduate School of Biomedical Sciences, 3601 4th Street, MS 9424, Lubbock, TX 79430, USA

*To whom correspondence should be addressed at: Garrison Institute on Aging, Cell Biology and Biochemistry, Neuroscience and Pharmacology and Neurology Departments, Texas Tech University Health Sciences Center, 3601 4th Street, MS 9424/4A 124, Lubbock, TX 79430, USA. Fax: 806-743-3636; Email: hemachandra.reddy@ttuhsc.edu

Abstract

The purpose of our study was to determine the toxic effects of hippocampal mutant APP and amyloid beta (Aβ) in 12-month-old APP transgenic mice. Using rotarod and Morris water maze tests, immunoblotting and immunofluorescence, Golgi-cox staining and transmission electron microscopy, we assessed cognitive behavior, protein levels of synaptic, autophagy, mitophagy, mitochondrial dynamics, biogenesis, dendritic protein MAP2 and quantified dendritic spines and mitochondrial number and length in 12-month-old APP mice that express Swedish mutation. Mitochondrial function was assessed by measuring the levels of hydrogen peroxide, lipid peroxidation, cytochrome c oxidase activity and mitochondrial ATP. Morris water maze and rotarod tests revealed that hippocampal learning and memory and motor learning and coordination were impaired in APP mice relative to wild-type (WT) mice. Increased levels of mitochondrial fission proteins, Drp1 and Fis1 and decreased levels of fusion (Mfn1, Mfn2 and Opa1) biogenesis (PGC1α, NRF1, NRF2 and TFAM), autophagy (ATG5 and LC3BI, LC3BII), mitophagy (PINK1 and TERT), synaptic (synaptophysin and PSD95) and dendritic (MAP2) proteins were found in 12-month-old APP mice relative to age-matched non-transgenic WT mice. Golgi-cox staining analysis revealed that dendritic spines are significantly reduced. Transmission electron microscopy revealed significantly increased mitochondrial numbers and reduced mitochondrial length in APP mice. These findings suggest that hippocampal accumulation of mutant APP and Aβ is

Received: December 22, 2017. **Revised:** January 12, 2018. **Accepted:** January 29, 2018

© The Author(s) 2018. Published by Oxford University Press. All rights reserved.
For permissions, please email: journals.permissions@oup.com

responsible for abnormal mitochondrial dynamics and defective biogenesis, reduced MAP2, autophagy, mitophagy and synaptic proteins and reduced dendritic spines and hippocampal-based learning and memory impairments, and mitochondrial structural and functional changes in 12-month-old APP mice.

Introduction

Alzheimer's disease (AD) is a progressive, heterogeneous, age-dependent, neurodegenerative disorder, characterized by the loss of memory, impairment of multiple cognitive functions and changes in the personality and behavior (1–4). Pathological examination of autopsied brains from patients with AD revealed that multiple cellular changes are associated with AD, including hyperphosphorylated tau and neurofibrillary tangles (NFTs), amyloid beta (Aβ) formation and accumulation, synaptic damage, loss of synapses, proliferation of reactive astrocytes and activated microglia, defects and alterations in cholinergic neurons and structural and functional changes in mitochondria (5–17). These changes were observed in learning and memory regions of the brain, including hippocampus and cortex. The involvement of Aβ is highly debated and still a central topic in AD pathogenesis, mainly because of its relevance to synaptic and mitochondrial damages and cognitive deficits.

Amyloid beta, a 4 kDa peptide is a major component of Aβ plaques found in AD brains. Recent molecular, cellular and animal model studies have provided evidence that Aβ—a product of APP due to the cleavage of β and γ secretases—is a key factor in AD development and progression (12). Aβ exists in multiple forms and the most prevalent forms of Aβ are Aβ40 and Aβ42, with Aβ42 being found to be the more highly toxic. Aβ42 is known to aggregate into accumulations of different sizes, ranging from monomeric to multimeric Aβ, and to participate in the formation of multimeric, diffusible, soluble aggregations, protofibrils, insoluble fibrils and Aβ deposits (12,18). The continuous production and reduced clearance of Aβ in neurons may lead to a cascade of events in the AD process (12). Several studies revealed that Aβ accumulations at synapses induce synaptic damage in AD neurons (13). However underlying precise cellular changes are not completely understood.

In healthy, intact synapses, synaptic terminals function actively to transmit signals between neurons and to process information (18–20). However, in elderly individuals and in AD patients and in elderly patients intact synaptic terminals exhibited changes that are responsible for cognitive decline (19–22). In a study of synaptic loss in the hippocampus (affected in AD), researchers found significant differences in the synapse-to-neuron ratio in samples taken from hippocampus of elderly patients with AD (19).

The loss of synapses and synaptic proteins that occurs before neuronal death in patients with AD appears to be accompanied by axonal degeneration and defective axonal transport of mitochondria (23–26). To explore the loss of synapses in AD neurons, Calkins *et al*. conducted an investigation of mRNA changes in synaptic genes of primary neurons from APP mice. This investigation of mRNA levels of synaptic genes in APP neurons revealed significantly reduced synaptic genes, suggesting that neurons that produce Aβ may also be deficient in synaptic mRNAs. They also found significantly reduced mitochondrial anterograde axonal transport in APP neurons (25). These results strongly suggest that synaptic degeneration and synaptic functional failure primarily due to defective mitochondria and malfunction of mitochondria in APP neurons. This research provides compelling evidence that Aβ-induced synaptic and mitochondrial damage plays a large role in cognitive decline in AD. However, hippocampal accumulation of mutant APP and/or Aβ causes defective synaptic mitochondria and altered dendritic spines are not completely understood. Further, how these hippocampal synaptic changes lead to cognitive decline are not completely understood.

In the current study, we sought to determine (1) hippocampal accumulation of mutant APP and Aβ, (2) hippocampal Aβ-induced dendritic spine loss and (3) the levels of dendritic protein MAP2, (4) changes in mitochondrial dynamics, biogenesis, synaptic and autophagy and mitophagy proteins, (5) mitochondrial structural and functional changes in the hippocampal region and (6) spatial learning and memory behavioral changes in 12-month-old APP transgenic mice (Tg2576 line) and age-matched non-transgenic WT mice.

Results

Cognitive behavior

Rotarod test

To determine whether mutant APP and Aβ affects motor coordination and motor skill acquisition, using rotarod, we assessed motor learning and coordination in 12-month-old APP and age-matched non-transgenic WT mice. Significantly reduced latency to fall on an accelerating rotarod test was observed in 12-month-old APP mice ($P = 0.002$) relative non-transgenic WT mice (Fig. 1A), indicating that the presence of impairments in motor learning and coordination. As shown in Figure 1A, the latency to fall in all four trails was consistent in APP mice, suggesting that impairments in motor learning and coordination was linked to mutant APP and Aβ.

Morris water maze test

Latency to find platform

To determine the hippocampal-dependent learning and memory in APP mice, we performed hidden-platform Morris water maze (MWA) test. APP mice showed an increase in escape latency to find the hidden platform during training between trials 4 and 16 relative to WT mice (Fig. 1B). The average latency time to find platform was significantly increased in APP mice ($P = 0.0001$) compared to non-transgenic WT mice. These observations indicate that the presence of an impairment of learning and memory in APP mice.

Swimming speed

To determine motor ability, we assessed the swimming speed in both APP and non-transgenic WT mice. As shown in Figure 1C, APP mice displayed a declined motor ability in MWA test, indicated by a gradually decreased swimming speed relative to WT mice. Average swimming speed was significantly decreased in APP mice ($P = 0.0001$) compared to WT mice.

Time spent in target quadrant

As shown in Figure 1D, during the probe trail, APP mice spent reduced time in all 16 trials on target quadrant compared to WT mice. Average time spent in target quadrant was significantly decreased in APP mice ($P = 0.0001$) compared to WT mice. These

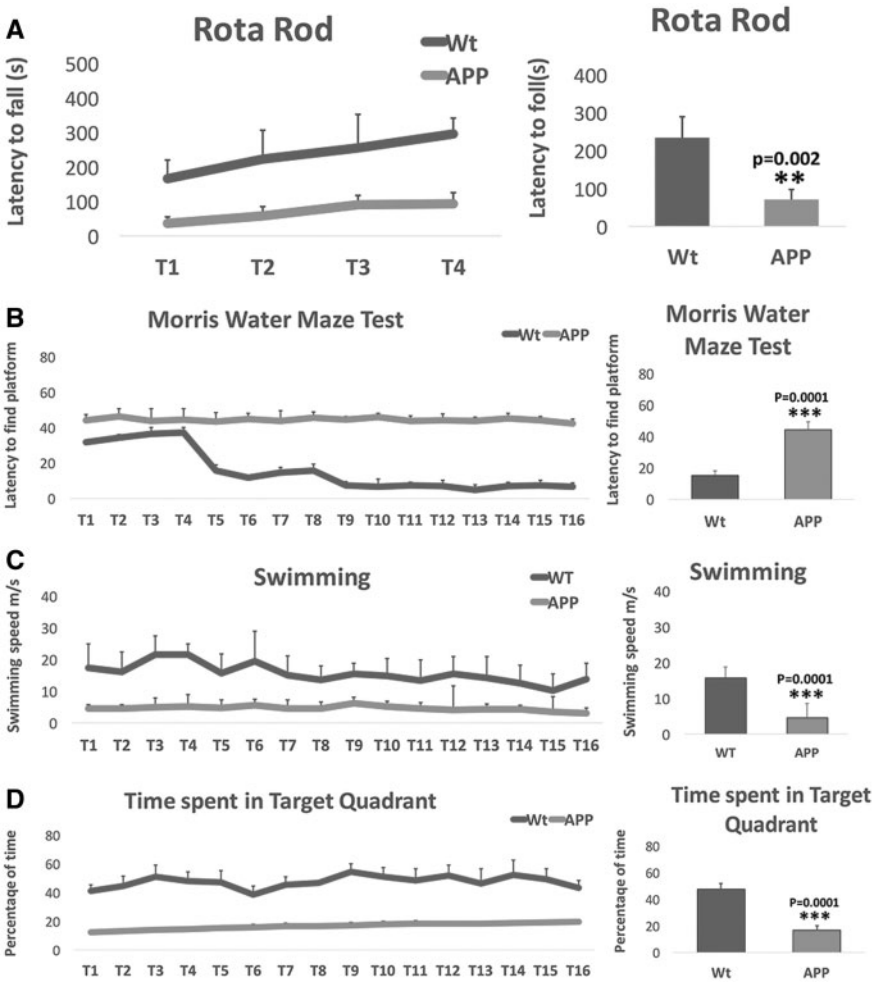

Figure 1. Cognitive behavior of 12-month-old APP and non-transgenic WT mice. (**A**) Represents rotarod test in 12-month-old APP mice ($n = 15$—8 males and 7 females) and non-transgenic WT mice ($n = 15$—8 males and 7 females). (**B**) Represents latency to find platform test in 12-month-old APP and non-transgenic WT mice. (**C**) Represents swimming speed in 12-month-old APP and non-transgenic WT mice. (**D**) Represents time spent target quadrant in 12-month-old APP and non-transgenic WT mice. *Rotarod.* Significantly reduced latency to fall on an accelerating rotarod test was found in 12-month-old APP mice ($P = 0.002$) relative to non-transgenic WT mice (A) and the latency to fall in all four trails was consistent in APP mice, suggesting that impairments in motor learning and coordination was progressive. *MWA test.* An increase in escape latency to find the hidden platform during training between trials 7 and 16 relative to WT mice and the average latency time to find platform was significantly increased in APP mice ($P = 0.0001$) compared to WT mice (B). *Swimming speed.* APP mice displayed a gradually decreased swimming speed relative to WT mice and an average swimming speed was significantly decreased in APP mice ($P = 0.0001$) compared to WT mice (C). *Target quadrant.* APP mice spent reduced time in all 16 trials on target quadrant compared to WT mice and average time spent in target quadrant was significantly decreased in APP mice ($P = 0.0001$) compared to WT mice (D).

observations strongly suggest that mutant APP and Aβ are responsible impairment in overall cognitive behavior.

Immunoblotting analysis

To understand the effects of mutant APP and Aβ on mitochondrial dynamics and mitochondrial biogenesis, we performed immunoblotting analysis of mitochondrial fission proteins, Drp1 and Fis1 and fusion proteins Mfn1, Mfn2 and Opa1 and biogenesis proteins PGC1α, NRF1, NRF2 and TFAM; synaptic proteins-synaptophysin and PSD95 and autophagy proteins ATG5, LC3BI and LC3BII and mitophagy proteins PINK1 and TERT in hippocampal tissues from 12-month-old APP and age-matched non-transgenic WT mice.

Mitochondrial dynamics proteins

As shown in Figure 2A and B, significantly increased levels of fission proteins Drp1 ($P = 0.002$) and Fis1 ($P = 0.02$) were found in hippocampal tissues from 12-month-old APP mice relative to age-matched WT mice. On the contrary, mitochondrial fusion proteins were significantly decreased fusion proteins, Mfn1 ($P = 0.04$), Mfn2 ($P = 0.001$) and Opa1 ($P = 0.04$) in hippocampal tissues from APP mice relative to WT mice. These observations indicate that accumulation of hippocampal mutant APP and Aβ caused impaired mitochondrial dynamics in APP mice.

Mitochondrial biogenesis

Significantly decreased levels of biogenesis proteins, PGC1α ($P = 0.01$), NRF1 ($P = 0.01$), NRF2 ($P = 0.005$) and TFAM ($P = 0.03$) were found in APP mice relative to non-transgenic WT mice, indicating that mitochondrial biogenesis was defective in APP mice (Fig. 2A and B).

Dendritic and synaptic protein MAP2

To determine the toxic effects of mutant APP and Aβ on dendritic protein, MAP2, and synaptic proteins, we quantified MAP2 and synaptophysin and PSD95 from hippocampal tissues of 12-month-

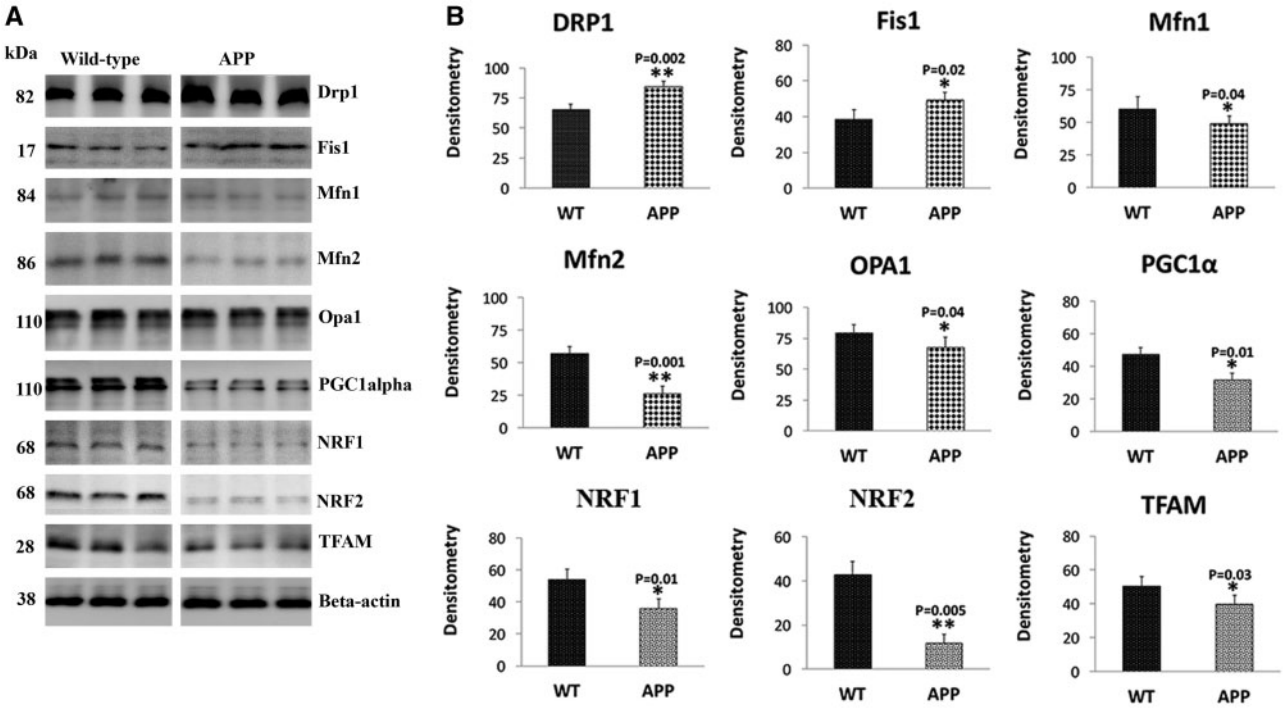

Figure 2. Immunoblotting analysis of mitochondrial dynamics proteins in 12-month-old APP and non-transgenic WT mice. (A) Shows representative immunoblotting analysis of 12-month-old APP mice. (B) Shows quantitative densitometry analysis of mitochondrial dynamics proteins Drp1, Fis1 (fission) and Mfn1, Mfn2 and Opa1 (fusion) and biogenesis protein PGC1α, NRF1, NRF2 and TFAM. Protein levels of Drp1 ($P = 0.002$), Fis1 ($P = 0.02$) were significantly increased; and Mfn1 ($P = 0.04$), Mfn2 ($P = 0.001$) and Opa1 ($P = 0.04$) were significantly decreased in APP mice relative to WT mice. Protein levels of PGC1α ($P = 0.01$), NRF1 ($P = 0.01$), NRF2 ($P = 0.005$) and TFAM ($P = 0.03$) were significantly decreased in APP mice relative to WT mice.

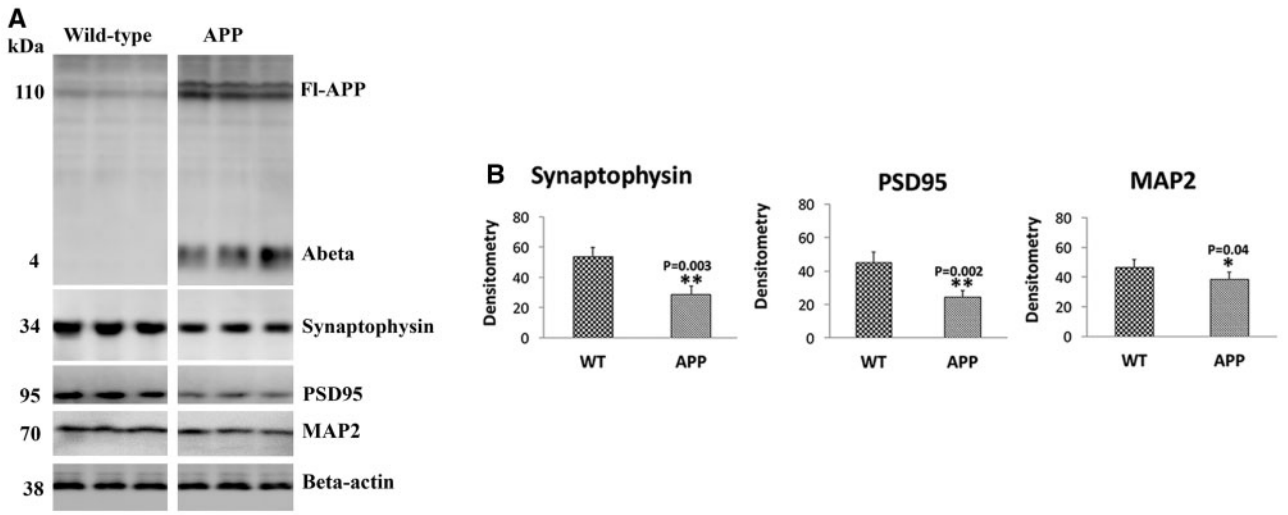

Figure 3. Immunoblotting analysis of synaptic and dendritic protein MAP2 in 12-month-old APP and non-transgenic WT mice. (A) Shows representative immunoblotting analysis of 12-month-old APP and WT mice. (B) Shows quantitative densitometry analysis of synaptic and MAP2 proteins. Synaptophysin ($P = 0.003$), PSD 95 ($P = 0.002$) and MAP2 ($P = 0.04$) were significantly decreased in APP mice relative to WT mice.

old APP and WT mice. In APP mice relative to WT mice, significantly decreased level of MAP2 ($P = 0.04$) was observed. As shown in Figure 3A and B, significantly decreased levels of synaptophysin ($P = 0.003$), PSD95 ($P = 0.002$) were found in 12-month-old APP mice relative to age-matched non-transgenic WT mice.

Autophagy and mitophagy proteins

Significantly decreased levels of autophagy proteins, ATG5 ($P = 0.01$), LC3BI ($P = 0.01$) and LC3BII ($P = 0.01$), and mitophagy proteins, PINK1 ($P = 0.02$), TERT was showed decreased level, but not significant, in APP mice relative to non-transgenic WT

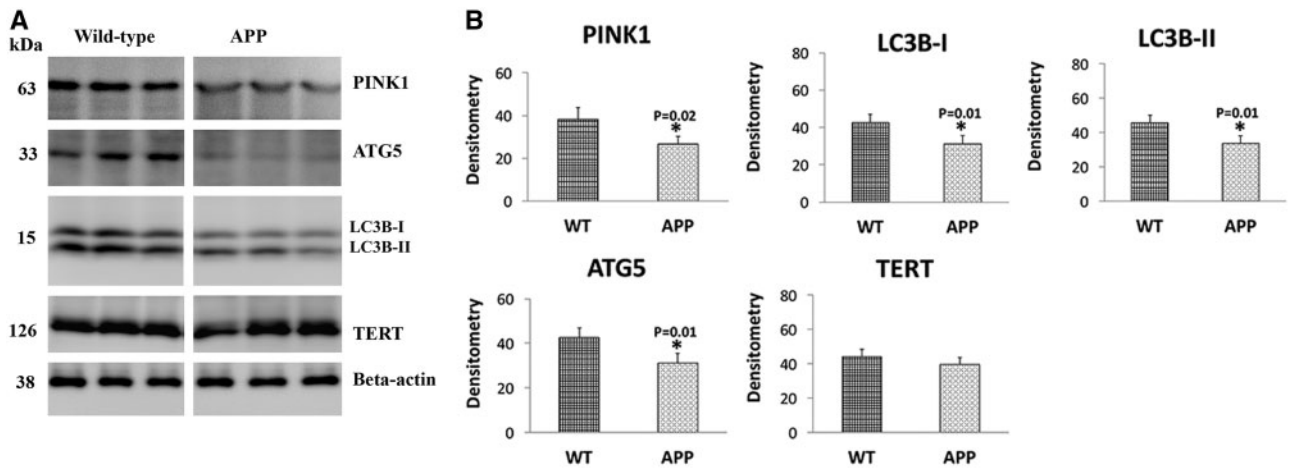

Figure 4. Immunoblotting analysis of autophagy and mitophagy proteins in 12-month-old APP and non-transgenic WT mice. (**A**) Shows representative immunoblotting analysis of 12-month-old APP and WT mice. (**B**) Shows quantitative densitometry analysis of autophagy proteins. PINK1 ($P = 0.02$), ATG ($P = 0.01$), LC3BI ($P = 0.01$), LC3BII ($P = 0.01$) and TERT were significantly decreased in APP mice relative to WT mice.

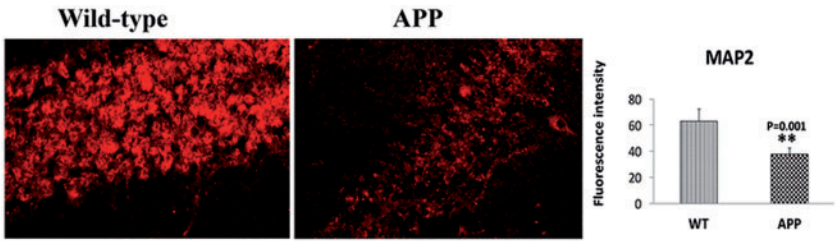

Figure 5. Immunofluorescence analysis of dendritic protein MAP2 protein in 12-month-old APP and non-transgenic WT mice. (**A**) Represents immunofluorescence analysis. (**B**) Represents quantitative immunofluorescence analysis. Significantly increased levels of MAP2 ($P = 0.001$) were found in 12-month-old APP mice relative to WT mice.

mice, indicating that autophagy was defective in APP mice (Fig. 4A and B).

Immunofluorescence analysis

Using immunofluorescence analysis, localizations and level of MAP2 protein was assessed in hippocampal sections from 12-month-old APP and WT mice.

As shown in Figure 5, significantly decreased levels of MAP2 ($P = 0.001$) were found in APP mice relative to WT mice, indicating that mutant APP reduces MAP2 in APP mice.

Dendritic spines

To determine the effects of mutant APP and Aβ on dendritic spines, we quantified dendritic spines using Golgi-cox staining in hippocampus of 12-month-old APP and age-matched non-transgenic WT mice.

As shown in Figure 6, we found significantly reduced dendritic spines in APP mice ($P = 0.0003$) relative to WT mice, indicating that mutant APP and Aβ reduces dendritic spines in APP mice.

Transmission electron microscopy

To determine the effects of mutant APP and Aβ on mitochondrial number and length, we used transmission electron microscopy on hippocampal and cortical tissues from 12-month-old APP mice and age-matched non-transgenic WT mice.

Mitochondrial number in hippocampus

As show in Figure 7A, we found significantly increased number of mitochondria in hippocampi of 12-month-old APP mice ($P = 0.0004$) relative to age-matched non-transgenic WT mice, suggesting that mutant APP and Aβ fragments hippocampal mitochondria.

Mitochondrial length in hippocampus

We also measured mitochondrial length in order to understand whether mutant APP and alters mitochondrial length. As shown in Figure 7A, we found mitochondrial length is significantly decreased in hippocampal tissues from APP mice ($P = 0.04$) relative to non-transgenic WT mice.

Mitochondrial number in cerebral cortex

As shown in Figure 7B, we found significantly increased number of mitochondria in cortical tissues of 12-month-old APP mice ($P = 0.0002$) relative to age-matched non-transgenic WT mice, suggesting that mutant APP and Aβ fragments cortical mitochondria.

Mitochondrial length in cerebral cortex

We also measured mitochondrial length in order to understand whether mutant APP and Aβ alters mitochondrial length. As shown in Figure 7B, we found that mitochondrial length is significantly decreased in cortical tissues from APP mice ($P = 0.02$) relative to WT mice.

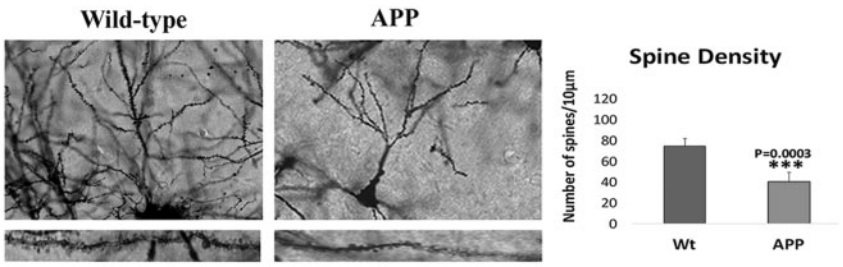

Figure 6. Hippocampal dendritic spine density in 12-month-old APP and non-transgenic WT mice. (A) Represents low magnification of Golgi-cox staining. (B) Represents enlarged neuron with dendrites and (C) represents quantification of spine density in APP and WT mice. Significantly reduced dendritic spines were found in APP mice ($P = 0.0003$) relative to WT mice, indicating that mutant APP and Aβ levels reduces dendritic spines in APP mice.

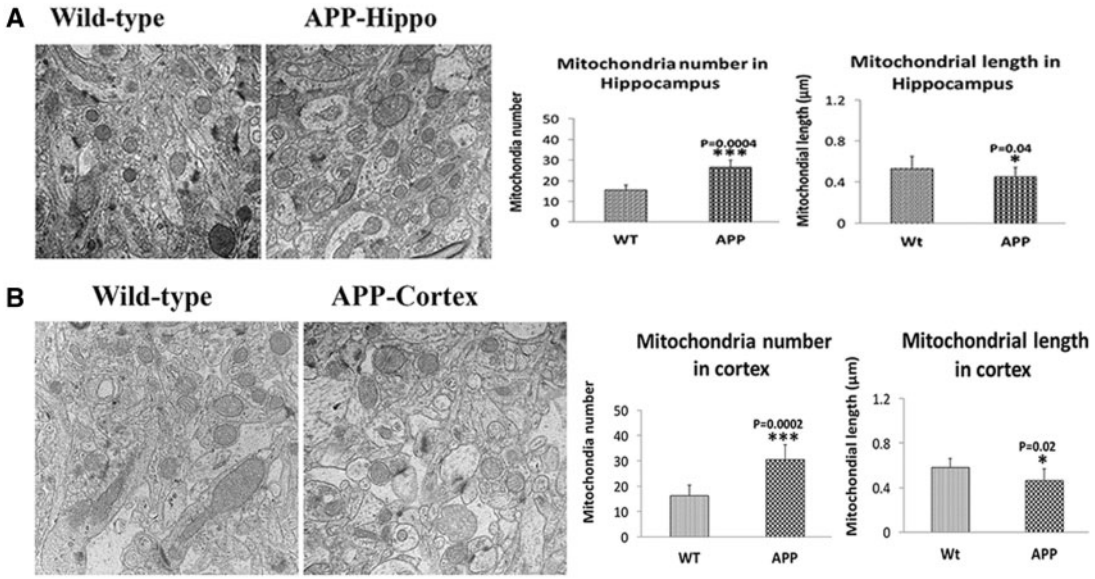

Figure 7. Mitochondrial number and length in 12-month-old APP and non-transgenic WT mice. (A) Represents mitochondrial number and length in hippocampus of APP mice and WT mice. (B) Represents mitochondrial number and length in cortex of APP and WT mice. Significantly increased number of mitochondria were found in the hippocampi of 12-month-old APP mice ($P = 0.0004$) relative to age-matched WT mice, suggesting that Aβ fragments hippocampal mitochondria. On the contrary, mitochondrial length is significantly decreased in the hippocampal tissues from APP mice ($P = 0.04$) relative to WT mice (A). Significantly increased number of mitochondria in cortical tissues of 12-month-old APP mice ($P = 0.0002$) relative to age-matched WT mice. Mitochondrial length is significantly decreased in cortical tissues from APP mice ($P = 0.02$) relative to WT mice.

Mitochondrial function

Mitochondrial function was assessed in hippocampus of 12-month-old APP mice and age-matched WT mice by measuring hydrogen peroxide, lipid peroxidation, cytochrome c oxidase activity and mitochondrial ATP.

H_2O_2 production

As shown in Figure 8A, significantly increased levels of hydrogen peroxide were found in 12-month-old APP mice relative to WT mice ($P = 0.001$), indicating that mutant APP and Aβ increases H_2O_2 levels in APP mice.

Lipid peroxidation

Similar to hydrogen peroxide, levels of 4-hydroxy-2-nonenol, an indicator of lipid peroxidation were significantly increased in APP mice ($P = 0.003$) relative to WT mice (Fig. 8B).

Cytochrome c oxidase activity

Significantly decreased levels of cytochrome oxidase activity were found in 12-month-old APP mice ($P = 0.001$) relative to WT mice (Fig. 8C), indicating that mutant APP and Aβ reduces cytochrome oxidase activity in APP mice.

ATP production

As shown in Figure 8D, significantly decreased levels of mitochondrial ATP were found in APP mice relative to WT mice ($P = 0.01$), indicating that mutant APP and Aβ affects mitochondrial ATP in APP mice.

Discussion

In the current study, we investigated the toxic effects of mutant APP/Aβ, including cognitive behavior, protein levels of autophagy, mitophagy synaptic, mitochondrial dynamics, biogenesis and dendritic protein MAP2, and levels of dendritic spines, mitochondrial number and length and mitochondrial function in 12-month-old APP mice and age-matched non-transgenic WT mice. We used rotarod and MWA tests, immunoblotting and immunofluorescence, Golgi-cox staining and transmission electron microscopy methods. Mitochondrial function was assessed by measuring the levels of hydrogen peroxide, lipid

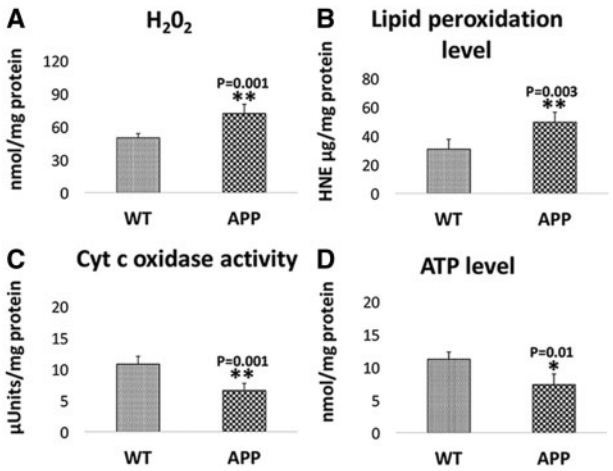

Figure 8. Mitochondrial functional parameters in 12-month-old APP and non-transgenic WT mice. Mitochondrial function was assessed by measuring: **(A)** H_2O_2 production, **(B)** lipid peroxidation, **(C)** cytochrome oxidase activity and **(D)** ATP levels. The levels of H_2O_2 ($P = 0.001$) and 4-hydroxy-2-nonenol ($P = 0.003$) were significantly increased and the levels of cytochrome oxidase ($P = 0.001$) and ATP ($P = 0.01$) significantly decreased found in APP mice relative to WT mice.

peroxidation, cytochrome *c* oxidase activity and mitochondrial ATP.

MWA and rotarod tests revealed that hippocampal learning and memory and motor learning and coordination were impaired in APP mice. Increased levels of mitochondrial fission proteins and decreased levels of mitochondrial fusion, biogenesis, autophagy, synaptic, proteins were found in 12-month-old APP mice relative to age-matched WT mice, indicating that the presence of abnormal mitochondrial dynamics and biogenesis, and defective synaptic, autophagy and dendritic proteins in APP mice. Mitochondrial dysfunction was defective. Golgi-cox staining analysis revealed that dendritic spines are significantly reduced. Transmission electron microscopy revealed significantly increased mitochondrial numbers and reduced mitochondrial length in APP mice. These findings suggest that mutant APP and Aβ are responsible for cognitive decline, altered levels of autophagy, mitophagy synaptic, mitochondrial dynamics, biogenesis and dendritic protein MAP2, and reduced dendritic spines and defective mitochondrial structural and functional changes.

Mutant APP and Aβ-induced abnormal cellular changes in AD

Impaired mitochondrial dynamics

Mutant APP and Aβ are reported to associate with mitochondria in AD neurons (12). Based on earlier mitochondria and Aβ studies, we proposed that the abnormal association of mutant APP/Aβ with mitochondria (via mitochondrial fission protein Drp1 interaction with Aβ) induces increased levels of GTPase Drp1 activity and causes excessive mitochondrial fragmentation (12,27–29). Our earlier studies of Drp1 interaction with Aβ and our current study findings from hippocampal tissues and mutant APP, further provided strong support with our hypothesis. Several recent studies from Zhu's group have provided compelling evidence to support our hypothesis that excessive mitochondrial fragmentation is an AD feature (26,30).

Defective mitochondrial biogenesis

The abnormal association of Aβ with mitochondria is proposed induce defective mitochondrial biogenesis in AD (22). Current study observations of reduced mitochondrial biogenesis proteins, including PGC1α, NRF1, NRF2 and TFAM in 12-month-old APP mice. Our current study observations agree with earlier studies in APP mice (31,32) and postmortem AD brains (33).

Defective autophagy/mitophagy

To understand the link between mutant APP/Aβ and mitochondria with autophagy and mitophagy—in the current study, we studied autophagy and mitophagy proteins in hippocampal tissues from APP mice. We found all autophagy ATG5, LC3BI and LC3BII and mitophagy PINK1 and TERT proteins were significantly reduced in hippocampal tissues from APP mice, indicating that abnormal accumulation of mutant APP and Aβ affects autophagy and mitophagy in hippocampal tissues in APP mice—in other words, full-length mutant APP and Aβ affects mitochondrial debris clearing mechanisms in AD. Our study findings of mitophagy agree with a recent study of Yan's group (13), further strengthening of our current study observations.

Reduced synaptic and dendritic proteins and reduced dendritic spines

Increasing evidence suggests that spine density is critical for synaptic function and cognitive behavior in AD patients and AD mice. In the current study, we assessed mutant APP and Aβ and spine density in 12-month-old APP transgenic mice. We found increased full-length mutant APP and 4 kDa Aβ in hippocampal tissues from APP mice. We also assessed the protein that is essential for dendritic growth—MAP2, in hippocampi of APP mice. We found robust levels of full-length mutant APP and 4 kDa Aβ in APP mice. We also found significantly reduced dendritic protein MAP2, and reduced levels of dendritic spines. Interestingly, as mentioned above, synaptic proteins synaptophysin and PSD95 were reduced. These changes in hippocampal tissues of APP mice, including increased full-length mutant APP and Aβ and reduced dendritic protein MAP2, reduced synaptic proteins and decreased spine density are undoubtedly responsible for synaptic damage and cognitive decline in APP mice.

Mitochondrial structural and functional changes

It is well-established that structurally damaged mitochondria are present in AD neurons and in the primary neurons from AD mice, particularly at nerve terminals (25). As discussed above, we found increased fission and decreased fusion proteins in 12-month-old APP mice, indicating that impaired mitochondrial dynamics is present in hippocampal tissues. These structurally damaged mitochondria are dysfunctional and may not produce ATP at synapses, leading to synaptic damage. To understand mitochondrial structural and functional changes, using transmission electron microscopy—we assessed mitochondrial number and length in hippocampal and cortical regions of APP mice. We found significantly increased number of mitochondria in hippocampal and cortical tissues of 12-month-old APP mice relative to age-matched WT mice, suggesting that mutant APP and Aβ accumulation fragments hippocampal and cortical mitochondria. As expected mitochondrial length was significantly decreased in hippocampal and cortical tissues from APP mice. Accumulation of mutant APP and Aβ is responsible for impaired mitochondrial dynamics (increased fission and decreased fusion) and mitochondrial structural abnormalities in APP mice.

Defective mitochondrial function

In APP mice, mitochondrial function was found to be defective. Lipid peroxidation and hydrogen peroxide levels were significantly increased in hippocampal tissues of the brain in APP mice. On the contrary, cytochrome oxidase activity and mitochondrial ATP were reduced in APP mice. It is interesting to note that the levels of mutant APP and Aβ are significantly increased in hippocampal tissues in APP mice, further strengthening our notion that mutant APP and Aβ responsible for mitochondrial and synaptic toxicities (reduced dendritic protein MAP2 and spine density) in APP mice.

Hippocampal mutant APP and Aβ-induced cognitive behavior

In the current study, we studied MWA primarily to understand the links between mutant APP and Aβ accumulation in hippocampus and spatial learning and memory in APP mice. As expected, APP mice exhibited longer time to reach the platform, which is considered to be a specific neurocognitive performance measure. Further, animals in swimming test, displayed decreased swimming speed in all 16 trials relative to WT mice. Average swimming speed was significantly decreased in APP mice compared to WT mice. Further, time spent in target quadrant is also reduced in APP mice. Average time spent in target quadrant was significantly decreased in APP mice compared to WT mice. Findings from these MWA test suggests that hippocampal accumulated APP is responsible for defects in spatial learning in APP mice.

On an accelerating rotarod test, APP mice displayed reduced latency to fall relative to non-transgenic WT mice, indicating that impairments in motor learning and coordination. The advantage of this test is that it creates a discretely measurable, continuous variable length of time that can be used to quantify the effects of accumulated mutant APP and Aβ in hippocampus mice.

Overall, these behavioral impairments together with increased levels of accumulated mutant APP and Aβ in hippocampus and reduced hippocampal dendritic spines, defective autophagy, abnormal mitochondrial dynamics, biogenesis and synaptic proteins strongly suggest that hippocampal mutant APP and Aβ accumulations are responsible for defective learning and memory and motor coordination in APP mice.

In summary, our study observations suggest that hippocampal accumulation of mutant APP and Aβ responsible for (1) cognitive impairments, (2) abnormal mitochondrial dynamics (increased fission and decreased fusion), (3) defective biogenesis, (4) reduced autophagy/mitophagy, (4) loss of dendritic protein MAP2, (5) dendritic spine density loss, (6) mitochondrial structural and functional changes, (7) synaptic damage and (8) neuronal dysfunction in APP mice. Our observations strongly suggest that reduced hippocampal Aβ is an important therapeutic strategy for AD.

Materials and Methods

Transgenic APP mice

Amyloid beta precursor protein mice (Tg2576 mice or APP) were generated with the mutant human APP gene 695 amino acid isoform and a double mutation ($Lys^{670}Asn$ and $Met^{671}Leu$) (Swedish mutation). This highly expressed human APP transgenic mouse line exhibits an age-dependent appearance of Aβ plaques, as well as confined distribution of these plaques to the cerebral cortex and the hippocampus, consistent with features of AD found in humans with AD. The APP mice show cognitive impairment at 6 months of age and older. The human APP transgene is maintained in the C57BL6/SJL background of these mice. To determine the mice that are transgene-positive for human APP, genotyping was performed, in accordance with the TTUHSC Policy on Genotype Tissue Collection, using the DNA prepared from tail biopsy and PCR amplification, as described in Manczak *et al.* (32). We used 15 ($n = 8$ males and $n = 7$ females) 12-month-old APP mice and 15 ($n = 8$ males and $n = 7$ females) age-matched non-transgenic WT mice for all the parameters studied in our paper.

Behavioral tests

Rotarod test

The general motor function was assessed by using a single mouse rotarod (MedAssociates, Inc.). The animals were placed on the rotarod one after the other facing away from the experimenter and the apparatus set to gradually increased from 2 to 40 rpm over the course of 300 s. When the animal falls, an IR beam is broken, stopping the motor and the timer. The time for each trial was recorded, with a maximum of 300 s. Mice were then removed and allowed to rest for 30 min until returning to the remaining two sessions of the test, yielding a total of three trials a day for three consecutive days. Evaluation was made by monitoring latency to fall and maximal rotation rate before the mouse fell down. A soft pad was placed under the equipment as a precautionary measure against physical damages from falls.

Morris water maze

The Morris water maze (MWM) apparatus (Coulborn Instruments, Allentown, PA) in our laboratory were based on the design of Richard Morris (1984) (28). This MWM was used to assess for studying different aspects of spatial memory (e.g. working memory); and non-spatial discrimination learning in APP mice with respect to the WT mice. The MWM apparatus consists of a 183 cm diameter pool filled with water to a depth of 48 cm and water temperature was maintained at 20°C. The platform (18 cm diameter) was placed in the pool approximately 2 cm below the surface of the water in one of the four quadrants. On the four sides of MWM apparatus different shapes of visual cues were placed inside the wall of the pool in a diagonal pattern. The water in the pool was made opaque to obscure the platform location using non-toxic white tempura paint (Utrecht Art Supplies, Cranbury, NJ). We used tracking software (Actimetrics, Wilmette, IL) to monitor and record each trial. In our MWM paradigm consisted of four 60 s trials per day for four consecutive days followed by reference memory probe trials after training. At end of each trial mouse was dried with dry cloth and retuned back to the home cage which was kept on heating pad. The interval for each trial mouse was approximately 10 min. For each trial, pre-determined starting position was different and allowed to swim while being tracked by the software. The trial ended when the animal found the platform or when 60 s had elapsed. If the mouse did not reach the platform, it was placed onto the platform and left there for 10 s. Reference memory probe trials consisted of a single 60 s free swim from a single start point. The platform was removed for the probe trial but its previous location was recorded with the monitoring software. A 60 s probe trial was performed on the fourth day to determine memory retention. For this single trial,

the submerged platform was removed and each mouse was placed into the quadrant opposite to the quadrant that formerly contained the platform in acquisition testing. The number of annulus crossings, the percentage of time spent in each quadrant and average swim speed was determined from the retrieved videotapes.

Immunoblotting analysis

To determine whether mutant APP and Aβ alters the protein levels of mitochondrial fission (Drp1 and Fis1) and fusion (Mfn1, Mfn2 and Opa1), biogenesis (PGC1α, NRF1, NRF2 and TFAM), dendritic protein, MAP2, synaptic proteins (synaptophysin and PSD95), autophagy (ATG5, LC3BI and LC3BII) and mitophagy (PINK1 and TERT), we performed immunoblotting analyses of protein lysates from 12-month-old APP, and WT mice as described in Manczak *et al*. (32). Twenty μg protein lysates from hippocampal tissues of all lines mice were resolved on a 4–12% Nu-PAGE gel (Invitrogen). The resolved proteins were transferred to nylon membranes (Novax Inc., San Diego, CA) and were then incubated for 1 h at room temperature with a blocking buffer (5% dry milk dissolved in a TBST buffer). The nylon membranes were incubated overnight with the primary antibodies (Drp1-1: 500 rabbit-polyclonal, Novus Biological, Littleton, CO; 1: 500 rabbit polyclonal of Fis1, Protein Tech Group, Inc., Chicago, IL; Mfn1-1: 400 rabbit polyclonal, Abcam, Cambridge, MA; Mfn2-1: 400 rabbit polyclonal, Abcam, Cambridge, MA; Opa1-1: 500 dilutions, BD Biosciences, San Jose, CA; MAP2-1: 500 dilutions, Santa Cruz Biotechnology, Dallas, TX; synaptophysin-1: 1000 dilutions, Novus Biological, Littleton, CO; PSD95-1: 1000 dilutions, Abcam, Cambridge, MA; PGC1α, NRF1, NRF2, TFAM, PINK1, ATG5, LC3B and TERT-1: 1000 dilutions, Novus Biological, Littleton, CO, USA). The membranes were washed with a TBST buffer three times at 10 min intervals and were then incubated for 2 h with appropriate secondary antibodies (1: 5000 dilutions of Anti mouse IgG HRP; Anti-rabbit IgG HRP, GE Health Care life Sciences, Pittsburgh, PA), followed by three additional washes at 10 min intervals. Proteins were detected with chemilumniscence reagents (Pierce Biotechnology, Rockford, IL), and the bands from immunoblots were quantified on a Kodak Scanner (ID Image Analysis Software, Kodak Digital Science, Kennesaw, GA). Briefly, image analysis was used to analyze gel images captured with a Kodak Digital Science CD camera. The lanes were marked to define the positions and specific regions of the bands. An ID fine-band command was used to locate and to scan the bands in each lane and to record the readings.

Immunofluorescence analysis and quantification of MAP2 and synaptic proteins in 12-month-old APP mice

Immunofluorescence analysis was performed using midbrain sections from APP, and WT mice as described in Manczak *et al*. (32). The midbrain sections APP and WT mice were washed with warm PBS, fixed in freshly prepared 4% paraformaldehyde in PBS for 10 min, and then washed with PBS and permeabilized with 0.1% Triton-X100 in PBS. They were blocked with a 1% blocking solution (Invitrogen) for 1 h at room temperature. All sections were incubated overnight with primary antibodies (1: 300 dilutions of MAP2, Santa Cruz Biotechnology, Dallas, TX). After incubation, the sections were washed three times with PBS, for 10 min each. The sections were incubated with a secondary antibody conjugated with Flours 594 (Ref# A21206, Molecular Probes, USA) 1 h at room temperature. The sections were washed three times with PBS and mounted on slides. Photographs were taken with a multiphoton laser scanning microscope system (ZeissMeta LSM510). To quantify the immunoreactivity of mitochondrial and synaptic antibodies for each treatment, 10–15 photographs were taken at × 40 magnifications, and statistical significance was assessed, using one-way ANOVA for proteins.

Golgi-cox staining and dendritic spine count

Golgi-cox impregnation has been one of the most effective techniques for studying both the normal and abnormal morphology of neurons. The morphology of neuronal dendrites and dendritic spines have been discovered in the brains of mice by using Golgi-cox staining and it was performed by using the FD Rapid Golgi-Cox Stain Kit (FD Neuro Technologies, Columbia, MD). Briefly, animals were anaesthetized before killing and brains from the mice skull were removed carefully as quickly as possible. The intact mice brain tissues were rinsed with Milli Q water to remove blood from the surface. The mice brain tissues were impregnated in the equal volumes of Solutions A and B, the impregnation solution was replaced the following day and stored at room temperature for 2 weeks in the dark. The brains were transferred to Solution C after 2 weeks. The Solution C was replaced the following day and the brains were stored at 4°C for 72 h in the dark. The Brain sections (100 μm thickness) were generated using a cryotome with the chamber temperature set at −22°C. Each section was mounted on gelatin-coated microscope slides using Solution C. The excess solution on slide was removed with a pasteur pipette and then absorbed with a stacks of filter paper and the sections were allowed to dry naturally at room temperature (3 days). The dried brain sections were processed as per the manufacturer's instructions. Briefly, dendrites within the CA1 sub region of the hippocampus were imaged using a 4×, 20× and, 40× and 64× objectives using EVOS microscope-AMG (thermofisher.com) and Olympus1X71. Dendritic spines were detected along CA1 secondary dendrites starting from their point of origin on the primary dendrite and the counting was performed by an experimenter blinded to the group of each sample (34,35).

Transmission electron microscopy

To determine the effects of mutant APP and Aβ on the mitochondrial number and size, we performed transmission electron microscopy in hippocampal and cortical sections of 12-month-old APP mice relative to age-matched WT mice. Animals were perfused using standard perfusion method. After successful perfusion, skin was removed on top of head and take the brain out, and post fixed the brain for 2–3 h and/or definitely, and cut the hippocampal and cortical sections for transmission electron microscopy. 1×1 mm thickness fixed sections from hippocampi and cortices were used for further analysis. Cut sections were stained for 5 min in lead citrate. They were rinsed and post-stained for 30 min in uranyl acetate and then were rinsed again and dried. Electron microscopy was performed at 60 kV on a Philips Morgagni TEM equipped with a CCD, and images were collected at magnifications of ×1 000–37 000. The numbers of mitochondria were counted per optic field and statistical significance was determined, using one-way ANOVA.

Mitochondrial functional assays

H_2O_2 production

Using an Amplex® Red Hydrogen Peroxide Assay Kit (Molecular Probes, Eugene, OR), the production of H_2O_2 was measured using hippocampal tissues from 12-month-old APP mice and WT mice as described in Kandimalla *et al.* (36). Briefly, H_2O_2 production was measured in the mitochondria hippocampal tissues from all four lines of mice. A BCA Protein Assay Kit (Pierce Biotechnology) was used to estimate protein concentration. The reaction mixture contained mitochondrial proteins (μg/μl), Amplex Red reagents (50 μM), horseradish peroxidase (0.1 U/ml) and a reaction buffer (1×). The mixture was incubated at room temperature for 30 min, followed by spectrophotometer readings of fluorescence (570 nm). Finally, H_2O_2 production was determined, using a standard curve equation expressed in nmol/μg mitochondrial protein. Hydrogen peroxide levels were compared between APP and mice.

Lipid peroxidation assay

Lipid peroxidates are unstable indicators of oxidative stress in the brain. The final product of lipid peroxidation is 4-hydroxy-2-nonenol (HNE), which was measured from hippocampal tissues from APP and WT mice. We used HNE-His ELISA Kit (Cell BioLabs, Inc., San Diego, CA) as described in Kandimalla *et al.* (32). Briefly, freshly prepared protein as added to a 96-well protein binding plate and incubated overnight at 4°C. It was then washed three times with a buffer. After the last wash, the anti-HNE-His antibody was added to the protein in the wells, which was then incubated for 2 h at room temperature and was washed again three times. Next, the samples were incubated with a secondary antibody conjugated with peroxidase for 2 h at room temperature, followed by incubation with an enzyme substrate. Optical density was measured (at 450nm) to quantify the level of HNE. Lipid peroxidation levels were compared between APP mice and WT mice.

Cytochrome oxidase activity

Cytochrome oxidase activity was measured in hippocampal tissues from APP and WT mice. Enzyme activity was assayed spectrophotometrically using a Sigma Kit (Sigma–Aldrich) following manufacturer's instructions (32). Briefly, 2 μg protein lysate was added to 1.1 ml of a reaction solution containing 50 μl 0.22 mM ferricytochrome c fully reduced by 0.1 M DTT, Tris–HCl (pH 7.0), and 120 mM potassium chloride. The decrease in absorbance at 550 mM was recorded for 1 min reactions at 10 s intervals. Cytochrome oxidase activity was measured according to the following formula: mU/mg total mitochondrial protein = (A/min sample − (A/min blank) × 1.1 mg protein × 21.84). The protein concentrations were determined following the BCA method. Cytochrome c oxidase activity levels were compared between APP mice and WT mice.

ATP levels

ATP levels were measured in mitochondria isolated from hippocampal tissues of APP and WT mice using ATP determination kit (Molecular Probes, USA) (36). The bioluminescence assay is based on the reaction of ATP with recombinant firefly luciferase and its substrate luciferin. Luciferase catalyzes the formation of light from ATP and luciferin. It is the emitted light that is linearly related to the ATP concentration, which is measured with a luminometer. ATP levels were measured from mitochondrial pellets using a standard curve method. ATP levels were compared between APP mice and WT mice.

Acknowledgements

We sincerely thank all the staff at the animal facility for taking care of all lines of mice that are used in the study.

Conflict of Interest statement. None declared.

Funding

Work presented in this paper was supported by NIH grants AG042178, AG047812 and NS105473, and the Garrison Family Foundation, CH Foundation and Alzheimer's Association SAGA grant (to P.H.R.).

References

1. Selkoe, D.J. (2001) Alzheimer's disease: genes, proteins, and therapy. *Physiol. Rev.*, **81**, 741–766.
2. Swerdlow, R.H., Burns, J.M. and Khan, S.M. (2010) The Alzheimer's disease mitochondrial cascade hypothesis. *J. Alzheimers Dis.*, **20**, S265–S279.
3. Reddy, P.H., Manczak, M., Mao, P., Calkins, M.J., Reddy, A.P. and Shirendeb, U. (2010) Amyloid-beta and mitochondria in aging and Alzheimer's disease: implications for synaptic damage and cognitive decline. *J. Alzheimers Dis.*, **20**, S499–S512.
4. Reddy, P.H., Tripathi, R., Troung, Q., Tirumala, K., Reddy, T.P., Anekonda, V., Shirendeb, U.P., Calkins, M.J., Reddy, A.P., Mao, P. *et al.* (2012) Abnormal mitochondrial dynamics and synaptic degeneration as early events in Alzheimer's disease: implications to mitochondria-targeted antioxidant therapeutics. *Biochim. Biophys. Acta*, **1822**, 639–649.
5. Nunomura, A., Perry, G., Aliev, G., Hirai, K., Takeda, A., Balraj, E.K., Jones, P.K., Ghanbari, H., Wataya, T., Shimohama, S. *et al.* (2001) Oxidative damage is the earliest event in Alzheimer disease. *J. Neuropathol. Exp. Neurol.*, **60**, 759–767.
6. Zhu, X., Perry, G., Smith, M.A. and Wang, X. (2013) Abnormal mitochondrial dynamics in the pathogenesis of Alzheimer's disease. *J. Alzheimers Dis.*, **33**, S253–S262.
7. Du, H., Guo, L., Yan, S., Sosunov, A.A., McKhann, G.M. and Yan, S.S. (2010) Early deficits in synaptic mitochondria in an Alzheimer's disease mouse model. *Proc. Natl Acad. Sci. U.S.A.*, **107**, 18670–18675.
8. McGeer, P.L. and McGeer, E.G. (1995) The inflammatory response system of brain: implications for therapy of Alzheimer and other neurodegenerative diseases. *Brain Res. Brain Res. Rev.*, **21**, 195–218.
9. Terry, R.D., Masliah, E., Salmon, D.P., Butters, N., DeTeresa, R., Hill, R., Hansen, L.A. and Katzman, R. (1991) Physical basis of cognitive alterations in Alzheimer's disease: synapse loss is the major correlate of cognitive impairment. *Ann. Neurol.*, **30**, 572–580.
10. DeKosky, S.T., Scheff, S.W. and Styren, S.D. (1996) Structural correlates of cognition in dementia: quantification and assessment of synapse change. *Neurodegeneration*, **5**, 417–421.
11. Swerdlow, R.H. (2011) Brain aging, Alzheimer's disease, and mitochondria. *Biochim. Biophys. Acta*, **1812**, 1630–1639.
12. Reddy, P.H. and Beal, M.F. (2008) Amyloid beta, mitochondrial dysfunction and synaptic damage: implications for

cognitive decline in aging and Alzheimer's disease. *Trends Mol. Med.*, **14**, 45–53.
13. Du, F., Yu, Q., Yan, S., Hu, G., Lue, L.F., Walker, D.G., Wu, L., Yan, S.F., Tieu, K. and Yan, S.S. (2017) PINK1 signalling rescues amyloid pathology and mitochondrial dysfunction in Alzheimer's disease. *Brain*, **140**, 3233–3251.
14. Fang, D., Wang, Y., Zhang, Z., Du, H., Yan, S., Sun, Q., Zhong, C., Wu, L., Vangavaragu, J.R., Yan, S. *et al.* (2015) Increased neuronal PreP activity reduces Aβ accumulation, attenuates neuroinflammation and improves mitochondrial and synaptic function in Alzheimer disease's mouse model. *Hum. Mol. Genet.*, **24**, 5198–5210.
15. Yu, Q., Fang, D., Swerdlow, R.H., Yu, H., Chen, J.X. and Yan, S.S. (2016) Antioxidants rescue mitochondrial transport in differentiated Alzheimer's disease trans-mitochondrial cybrid cells. *J. Alzheimers Dis.*, **54**, 679–690.
16. Yu, Q., Du, F., Douglas, J.T., Yu, H., Yan, S.S. and Yan, S.F. (2017) Mitochondrial dysfunction triggers synaptic deficits via activation of p38 MAP kinase signaling in differentiated Alzheimer's disease trans-mitochondrial cybrid cells. *J. Alzheimers Dis.*, **59**, 223–239.
17. Wang, W., Yin, J., Ma, X., Zhao, F., Siedlak, S.L., Wang, Z., Torres, S., Fujioka, H., Xu, Y., Perry, G. and Zhu, X. (2017) Inhibition of mitochondrial fragmentation protects against Alzheimer's disease in rodent model. *Hum. Mol. Genet.*, **26**, 4118–4131.
18. Tampellini, D. and Gouras, G.K. (2010) Synapses, synaptic activity and intraneuronal abeta in Alzheimer's disease. *Front. Ag. Neurosci.*, **2**, 13–21.
19. Bertoni-Freddari, C., Fattoretti, P., Casoli, T., Caselli, U. and Meier-Ruge, W. (1996) Deterioration threshold of synaptic morphology in aging and senile dementia of Alzheimer's type. *Anal. Quant. Cytol. Histol.*, **18**, 209–213.
20. Hyman, B.T., Van Hoesen, G.W., Kromer, L.J. and Damasio, A.R. (1986) Perforant pathway changes and the memory impairment of Alzheimer's disease. *Ann. Neurol.*, **20**, 472–481.
21. Scheff, S.W., Anderson, K.J. and DeKosky, S.T. (1985) Strain comparison of synaptic density in hippocampal CA1 of aged rats. *Neurobiol. Aging*, **6**, 29–34.
22. Scheff, S.W., Scott, S.A. and DeKosky, S.T. (1991) Quantitation of synaptic density in the septal nuclei of young and aged Fischer 344 rats. *Neurobiol. Aging*, **12**, 3–12.
23. Reddy, P.H., Mani, G., Park, B.S., Jacques, J., Murdoch, G., Whetsell, W., Jr, Kaye, J. and Manczak, M. (2005) Differential loss of synaptic proteins in Alzheimer's disease: implications for synaptic dysfunction. *J. Alzheimers Dis.*, **7**, 103–117.
24. Almeida, C.G., Tampellini, D., Takahashi, R.H., Greengard, P., Lin, M.T., Snyder, E.M. and Gouras, G.K. (2005) Beta-amyloid accumulation in APP mutant neurons reduces PSD-95 and GluR1 in synapses. *Neurobiol. Dis.*, **20**, 187–198.
25. Calkins, M.J., Manczak, M., Mao, P., Shirendeb, U. and Reddy, P.H. (2011) Impaired mitochondrial biogenesis, defective axonal transport of mitochondria, abnormal mitochondrial dynamics and synaptic degeneration in a mouse model of Alzheimer's disease. *Hum. Mol. Genet.*, **20**, 4515–4529.
26. Wang, X., Su, B., Lee, H.G., Li, X., Perry, G., Smith, M.A. and Zhu, X. (2009) Impaired balance of mitochondrial fission and fusion in Alzheimer's disease. *J. Neurosci.*, **29**, 9090–9103.
27. Reddy, P.H. (2009) Amyloid beta, mitochondrial structural and functional dynamics in Alzheimer's disease. *Exp. Neurol.*, **218**, 286–292.
28. Manczak, M., Calkins, M.J. and Reddy, P.H. (2011) impaired mitochondrial dynamics and abnormal interaction of amyloid beta with mitochondrial protein Drp1 in neurons from patients with Alzheimer's disease: implications for neuronal damage. *Hum. Mol. Genet.*, **20**, 2495–2509.
29. Manczak, M. and Reddy, P.H. (2012) Abnormal interaction between the mitochondrial fission protein Drp1 and hyperphosphorylated tau in Alzheimer's disease neurons: implications for mitochondrial dysfunction and neuronal damage. *Hum. Mol. Genet.*, **21**, 2538–2547.
30. Wang, X., Su, B., Siedlak, S.L., Moreira, P.I., Fujioka, H., Wang, Y., Casadesus, G. and Zhu, X. (2008) Amyloid-beta overproduction causes abnormal mitochondrial dynamics via differential modulation of mitochondrial fission/fusion proteins. *Proc. Natl. Acad. Sci. U.S.A.*, **105**, 19318–19323.
31. Sheng, B., Wang, X., Su, B., Lee, H.G., Casadesus, G., Perry, G. and Zhu, X. (2012) Impaired mitochondrial biogenesis contributes to mitochondrial dysfunction in Alzheimer's disease. *J. Neurochem.*, **120**, 419–429.
32. Manczak, M., Kandimalla, R., Fry, D., Sesaki, H. and Reddy, P.H. (2016) Protective effects of reduced dynamin-related protein 1 against amyloid beta-induced mitochondrial dysfunction and synaptic damage in Alzheimer's disease. *Hum. Mol. Genet.*, **25**, 5148–5166.
33. Morris, R. (1984) Developments of a water-maze procedure for studying spatial learning in the rat. *J. Neurosci. Methods*, **11**, 47–60.
34. Gibb, R. and Kolb, B. (1998) A method for vibratome sectioning of Golgi-Cox stained whole rat brain. *J. Neurosci. Methods*, **79**, 1–4.
35. Kandimalla, R., Manczak, M., Yin, X., Wang, R. and Reddy, P.H. (2017) Hippocampal phosphorylated tau induced cognitive decline, dendritic spine loss and mitochondrial abnormalities in a mouse model of Alzheimer's disease. *Hum. Mol. Genet.*, **27**, 30–40.
36. Kandimalla, R., Manczak, M., Fry, D., Suneetha, Y., Sesaki, H. and Reddy, P.H. (2016) Reduced dynamin-related protein 1 protects against phosphorylated Tau-induced mitochondrial dysfunction and synaptic damage in Alzheimer's disease. *Hum. Mol. Genet.*, **25**, 4881–4897.